Eur. Phys. J. E (2020) **43**: 61
DOI 10.1140/epje/i2020-11986-3

THE EUROPEAN PHYSICAL JOURNAL E

Regular Article

Experimental and theoretical investigations on thermal conductivity of a ferrofluid under the influence of magnetic field

Catalin N. Marin and Iosif Malaescu[a]

West University of Timisoara, Faculty of Physics, Bd. V. Parvan nr. 4, 300223 Timisoara, Romania

Received 23 April 2020 / Received in final form 20 August 2020 / Accepted 3 September 2020
Published online: 29 September 2020

Abstract. The effect of the strength and orientation of magnetic field with respect to the temperature gradient on the effective thermal conductivity $\lambda_{eff}(H)$, in a kerosene-based ferrofluid with magnetite particles is reported. A new theoretical model to explain the experimental dependence $\lambda_{eff}(H)$, obtained for both the parallel and perpendicular orientation of the magnetic field, relative to the temperature gradient is proposed, based on the Sillars equation (which is applied for the first time to a ferrofluid in this purpose). For computing λ_{theor}, we have considered that the particle agglomerations, arranged in field-induced microstructures, have ellipsoid forms and the ratio a/b between the major axis and the minor axis of the ellipsoid increases with increasing the magnetic field strength. Using the proposed theoretical model, we established for the first time a semi-empirical relationship between the ratio, a/b and the magnetic field, H, both for parallel and perpendicular H relative to the temperature gradient, determining then the dependence on H of λ_{theor}. The theoretical results are in agreement with the experimental measurements. The reported results are of great practical importance and show that ferrofluids may be useful for incorporation in magnetic tuneable heat transfer devices or for other potential thermal applications.

1 Introduction

The solid-liquid biphasic systems have been used to enhance the transfer of heat through fluids. In order to prevent sedimentation of the solid particles, they were coated with a surfactant and their size was reduced to the nanometer order. Such biphasic fluids are called nanofluids [1], having higher heat transfer performance compared to the usual fluids [2] and which can be used in industrial applications based on the heat transfer [3].

A special category of nanofluids is that of magnetic fluids, or ferrofluids, which are ultra-stable colloidal systems consisting of magnetic nanoparticles dispersed in a carrier liquid and stabilized with a suitable surfactant, the diameter of particles ranging from approximately 2 to 15 nm [4]. Unlike non-magnetic nanofluids, some of the ferrofluids have the property that in the presence of a static magnetic field, the magnetic nanoparticles form agglomerates in the shape of elongated droplets, along the direction of the magnetic field [5]. The length of the elongated droplets can reach the value of hundreds of micrometers and these so-called droplets vanish after the magnetic field removal [5]. Recent studies on the formation of ferrofluid droplets from a nozzle, in the presence of a non-uniform varying magnetic field [6], or in DC and AC magnetic field, for different angles of the magnetic coil axis with respect to gravity field [7,8] were reported. The results have shown that at an angle of 45°, the diameter of droplets has a minimum value, both in the DC and AC magnetic field [7,8].

In the last years, the experimental and theoretical studies of the thermal properties of ferrofluids (the thermal conductivity, viscosity, diffusivity, etc.) were an intense research topic, due to potential applications in heat transfer and cooling of electronic devices [9–11], the enhancement of boiling heat transfer [12], magnetic data storage, thermally conductive films, interference shielding, new sensors, etc. [13].

Using the transient hot-wire method, Quiang Li *et al.* [9] investigated the effect of the magnetic field, oriented both parallel and perpendicular to the temperature gradient, on the thermal conductivity of a Fe-water magnetic fluid. They found that the thermal conductivity of the ferrofluid is larger than that of carrier liquid, both in the absence and in the presence of the parallel magnetic field, attributing this increase to particle agglomerations. In the configuration of magnetic field perpendicular to the temperature gradient, very small changes in the thermal conductivity were observed.

John Philip *et al.* [10] observed a 300% increase of the thermal conductivity in a nanofluid consisting of

[a] e-mail: iosif.malaescu@e-uvt.ro (corresponding author)

magnetite particles dispersed in kerosene, when subjected to a magnetic field oriented parallel to the temperature gradient. The thermal conductivity of samples was measured using a thermal property analyzer [10]. They assigned this increase of thermal conductivity to the effective conduction of heat through the chainlike structures formed in the nanofluid sample in the presence of the magnetic field. By applying a perpendicular magnetic field to the direction of heat flux, Vinod *et al.* [14] did not observe a significant enhancement in the thermal transport. Recent results obtained by Sithara Vinod *et al.* [15], for polydisperse systems containing magnetite particles, show an increase in thermal conductivity of 180% for 17 G/s ramp rate at 200 G and of 230% for 33 G/s ramp. Alternating magnetic field cycles and faster field ramps were found to be helpful in improving the thermal transport of ferrofluids [15].

Anwar Gavili *et al.* [11] measured the thermal conductivity of a water-based ferrofluid with magnetite (Fe_3O_4) particles, with a volume fraction of 5.0% and an average diameter of 10 nm. The test sample of the ferrofluid was introduced in a stainless-steel box through which water circulates at different temperatures and which was in a magnetic field perpendicular to the sample, produced by the Helmholtz coils [11]. According to their results, by increasing the intensity of magnetic field to 1000 G, the ferrofluid has a thermal conductivity up to 200% higher than the value measured in the absence of the magnetic field and this increase was attributed to the formation of particle chains.

Some theoretical models have been developed for the effective thermal conductivity of a colloidal system [16,17] in zero polarizing fields. Thus, the Maxwell model predicts the thermal conductivity of a solid-liquid mixture, with spherical nanoparticles [18], at low volume fraction. The Bruggeman model [19] takes into account the interaction between the randomly distributed spherical nanoparticles and it matches well with the Maxwell model for low volume fraction of particles. Wang *et al.* [20] developed a theoretical model by modifying the Maxwell model, suggesting that the reason for the increase of the thermal conductivity of ferrofluids is related to the effects of the double electric layer and of the Van der Walls force, which could lead to the strong electrokinetic effects on nanoparticles. The Hamilton-Crosser [21,22] model is a modification of the Maxwell model, which also takes into account the particle shape, by including a form factor ($n = 3$ for spherical particles and $n = 6$ for particles of cylindrical shape).

The applied magnetic field can have various orientations with respect to the temperature gradient in the ferrofluid sample, it can be uniform or as a field gradient, thus resulting in a variety of configurations in which the magnetic field can affect the heat transfer through a ferrofluid. The theoretical models regarding the effect of the magnetic field on the thermal conductivity of ferrofluids are very few in literature. Recently, Susan Mousavi *et al.* [23] have proposed a semi-empirical theoretical model that includes a compression function dependent on the particle concentration and can explain the increase of the thermal conductivity of a ferrofluid in the presence of the parallel magnetic field. Dong-Sing Song *et al.* [24] have developed a computer simulation model based on phonons transport to estimate the anisotropic thermal conductivity in ferrofluid, assuming chain-like aggregation of particles in the presence of the magnetic field. The model is valuable only in the cases of small size and low particle concentration.

In the present paper, unlike other authors, the effective thermal conductivity, λ_{eff}, of a kerosene-based ferrofluid was determined using the conventional thermal conduction method [20,25]. This method has the advantage that, in performing the experiment, the tube containing the ferrofluid sample was placed in a horizontal position, in order to reduce the effect of convection on the measured values of λ_{eff}. One end of the tube is in contact with a hot source (T_1), whilst the other end is in contact with the cold source (T_2), measuring the time dependence of the temperature difference between the two ends, *i.e.* the heat transfer by ferrofluid sample. Simultaneously, using this method, we were able to track the effect of an external magnetic field, H, oriented both parallel and perpendicular relative to the direction of the temperature gradient on the effective thermal conductivity of ferrofluid, measuring both of $\lambda_{eff,II}(H)$ and $\lambda_{eff,\perp}(H)$.

To explain the experimental dependence $\lambda_{eff}(H)$, obtained for both the parallel and perpendicular orientation of the magnetic field with respect to the temperature gradient, we have proposed a new theoretical model based on the Sillars equation [26,27]. For this, we have considered that the particle agglomerations, arranged in field-induced microstructures, have ellipsoid forms and the ratio a/b between the major axis and the minor axis of the ellipsoid increases with the increase of the magnetic field strength. Based on the experimental values of thermal conductivity $\lambda_{eff}(H)$ and using the proposed theoretical model, we established for the first time a semi-empirical relationship between the ratio a/b and the magnetic field H, both for parallel and perpendicular orientation of the field with respect to the temperature gradient.

2 Sample characterization

For measurements, we have used a ferrofluid sample consisting of magnetite particles dispersed in kerosene and stabilized with oleic acid, having a density $\rho_F = 1240\,\mathrm{kg/m^3}$. The magnetite nanoparticles were obtained by chemical co-precipitation of bivalent and trivalent iron salts with an excess of NH_4OH in aqueous solution [28]. The stabilization of the particles was done by hydrofobization in the absence of the dispersion medium and finally, the resulting magnetic material was dispersed in kerosene. After the particle dispersion in kerosene, the ferrofluid was filtered in a magnetic field gradient to remove aggregates and coarse particles [28,29].

The investigated ferrofluid sample has the specific feature that when subjected to a static magnetic field, the magnetic nanoparticles form large agglomerates, elongated on the direction of the magnetic field. This characteristic of the ferrofluid sample was proven by magneto-optical investigation [29], for similar ferrofluid samples.

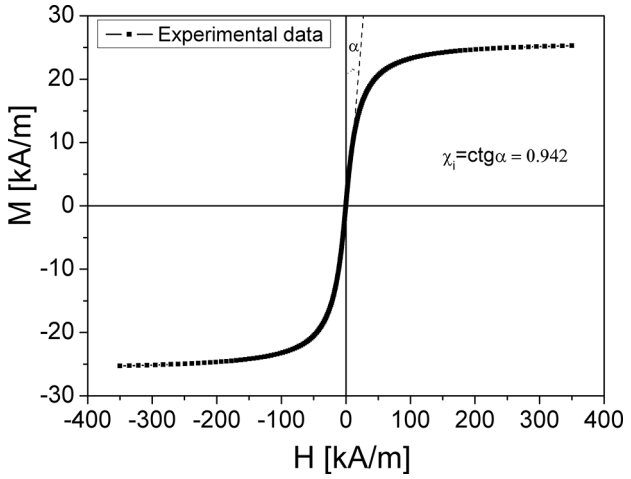

Fig. 1. The dependence of the magnetization, M, on the magnetic field, H, of the ferrofluid sample.

The magnetic characterization of the ferrofluid sample was performed at a low-frequency driving field (50 Hz), by means of an induction hysteresisgraph [30]. Figure 1 shows the magnetic field dependence, H, of the magnetization, M, of the sample.

As can be seen in fig. 1, the $M(H)$ dependence has the form of a Langevin-type law. Based on the experimental dependence $M(H)$ and using the Chantrell method of magneto-granulometric analysis [31], we have determined the following parameters: the saturation magnetization of the ferrofluid sample (M_∞), the mean magnetic diameter of particles (d_m), the standard deviation (SD) of the log-normal particle size distribution, the particle concentration (n) and the initial susceptibility (χ_i). The following values were obtained: $M_\infty = 26.10\,\mathrm{kA/m}$; $d_m = 11.50\,\mathrm{nm}$; $SD = 1.55\,\mathrm{nm}$; $n = 8.60 \cdot 10^{22}\,\mathrm{m}^{-3}$ and $\chi_i = 0.942$. The volume fraction of the magnetic phase (φ_m) from the ferrofluid was determined with the relation, $\varphi_m = \frac{M_\infty}{M_S}$ [4], where $M_S = 477.5\,\mathrm{kA/m}$ is the spontaneous magnetization of the bulk material from which the magnetite particles originate and the obtained value is $\varphi_m = 5.50\%$.

As is known [4], due to the chemical reaction between the oleic acid and magnetite, a thin shell of chelate is formed on the surface of each magnetite particle. However, for thermal transfer, the entire solid phase is important and its volume fraction should be taken into account. The volume fraction of the magnetic phase, φ_m, is correlated to the volume fraction of the entire solid phase, φ, by the relation, $\varphi = \varphi_m(1 + \frac{2\delta}{d_m})^3$, where δ represents the thickness of the non-magnetic shell (usually taken of the same value as the unit cell of the material of particles, *i.e.* 0.84 nm for magnetite) [4]. The above equation was used to compute the volume fraction of the entire solid phase, the value obtained being, $\varphi = 8.20\%$.

3 The experimental setup

The transient hot wire method is usually involved in the thermal conductivity of fluids, but in the case of ferrofluids it may induce particle agglomerations, that alter the result. Here, measurements of λ_{eff} were made using the conventional thermal conduction method [32], by means of a laboratory experimental setup, as shown schematically in fig. 2. Details on the field-induced microstructures (particle agglomerations) formed in the ferrofluid sample, in the presence of the applied magnetic field, are also illustrated. The experimental configuration of fig. 2 consists of a thermally insulated glass tube, of length L and cross-sectional area S, in which the ferrofluid sample is contained. In order to reduce the effect of convection on the measured values of λ_{eff}, the glass tube was placed horizontally. One end of the tube is in contact with a hot source (T_1), whilst the other end is in contact with the cold source (T_2). The contact with the hot source is achieved by a copper plate, which is fixed to one end of the tube and is in contact with an electric heater by means of which it can raise the temperature (T_1) to the desired value. The cold end is also in contact with a copper plate. The temperatures T_1 and T_2 were measured using thermocouples connected to the plates at the ends of the measuring tube. The measuring tube, containing the ferrofluid sample, is placed either in the magnetic field, H_{II} (parallel to the axis of the tube) (fig. 2(a)), or in the magnetic field $H_\perp$, (perpendicular to the axis of the tube) (fig. 2(b)).

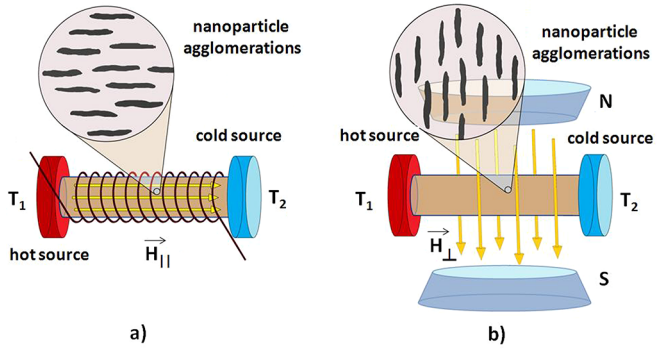

Fig. 2. The experimental setup: (a) the magnetic field, H_{II}, is parallel to the axis of the tube and (b) the magnetic field, $H_\perp$, is perpendicular to the axis of the tube.

The parallel magnetic field, H_{II}, has been produced into a magnetization coil whose field constant is $k = 3.57 \cdot 10^4\,\mathrm{m}^{-1}$. The magnetic coil is made on an ebonite tube of circular section, having a diameter of 12 mm and a length of 10 cm, by winding with copper wire of 1 mm diameter and 151 m in length. The perpendicular magnetic field $H_\perp$ has been produced into a electromagnet with the adjustable distance between the its poles. Both magnetic coil and the poles of the electromagnet are connected to a DC power supply. The values of the magnetic flux density in the centreline of the magnetic coil and the centreline of the electromagnet, respectively, were measured with a gauss-meter (HT20-EuroMagnet) with an error of 0.01 mT, for different values of the electrical current from the magnetization coil.

The thermal power, P_{th}, transmitted from the hot source to the cold source is given by the equation [32]

$$P_{th} = C \left| \frac{\mathrm{d}(\Delta T)}{\mathrm{d}t} \right|, \qquad (1)$$

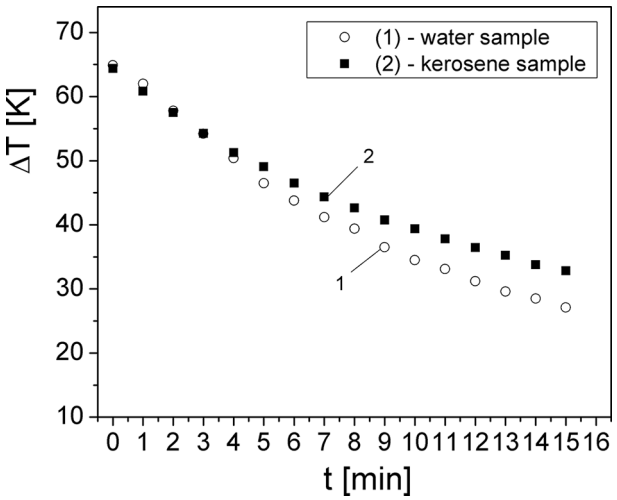

Fig. 3. Plot of the variation of temperature difference between the hot end and the cold end of the samples, ΔT, against time, t, (both for kerosene and for water).

where ΔT is the temperature difference between the hot end and the cold end of the sample ($\Delta T = T_1 - T_2$), $\mathrm{d}(\Delta T)/\mathrm{d}t$ is the time derivative of temperature difference between the hot end and the cold end of the sample and C is the heat capacity of copper. The relationship between thermal power and thermal conductivity is given by [32]

$$C\left|\frac{\mathrm{d}(\Delta T)}{\mathrm{d}t}\right| = \lambda_{eff}\Delta T\frac{S}{L}, \qquad (2)$$

where λ_{eff} is the effective thermal conductivity of the sample. Thus knowing the time dependence of the temperature difference between the hot end and the cold end of the sample, λ_{eff} can be determined from eq. (2).

The test of the experimental installation was made using kerosene and water, whose thermal conductivities reported in the literature are $\lambda_{wat} = 0.613\,\mathrm{W/K\cdot m}$ (water) [33] and $\lambda_{ker} = 0.15\,\mathrm{W/K\cdot m}$ (kerosene) [34]. Both for water and kerosene samples, the temperatures T_1 and T_2 (from opposite ends of the tube) were recorded at one-minute intervals, over the time interval, $\Delta t = 15\,\mathrm{min}$ and the results obtained are shown in fig. 3.

Based on the experimental results from fig. 3, for each sample, the time derivative of temperature difference between the hot end and the cold end of the sample ($\mathrm{d}(\Delta T)/\mathrm{d}t$) was determined. Using eq. (2) the thermal conductivity of the water and kerosene samples were computed and the results obtained were $\lambda_{wat}(\mathrm{exp}) = 0.628\,\mathrm{W/K\cdot m}$ and $\lambda_{ker}(\mathrm{exp}) = 0.145\,\mathrm{W/K\cdot m}$, respectively. These experimental values compare favourably with the values given in refs. [33] and [34]. This fact confirms that the experimental arrangement of fig. 2 can be successfully used to determine the thermal conductivity of ferrofluids.

4 Results and discussions

4.1 Experimental results

In order to study the heat transfer through the ferrofluid sample, the time (t) dependence of the temperature difference, $\Delta T = T_1 - T_2$, between the two ends of the sample has been measured, both in the absence of the magnetic field and when the field is applied perpendicularly ($H_\perp$) or parallel (H_{II}) to the temperature gradient. The obtained results for the ferrofluid sample, in comparison with the basic liquid of the investigated ferrofluid (*i.e.* kerosene), are presented in fig. 4.

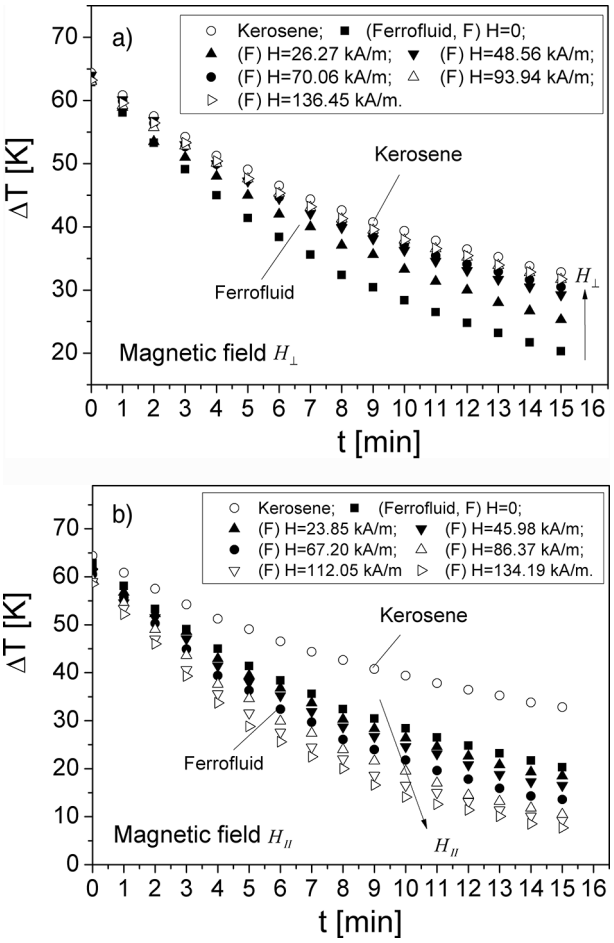

Fig. 4. Time dependence (t) of the temperature difference (ΔT) between the hot end and the cold end of the ferrofluid sample, in the presence of the magnetic field perpendicular $H_\perp$ (a) and parallel H_{II} (b) to the temperature gradient.

From fig. 4, the time derivative of temperature difference between the hot and the cold ends of the sample was computed and then, using eq. (2), λ_{eff} of the ferrofluid was determined, for each value of the applied magnetic field.

The dependence on the magnetic field of the obtained values for the effective thermal conductivity, $\lambda_{eff}(H)$, of the ferrofluid sample both in the case of perpendicular $H_\perp$ and parallel H_{II} magnetic field in relation to the temperature gradient is shown in fig. 5. The relative error in the measurement of the effective thermal conductivity was $\pm 4.4\%$.

As can be seen from fig. 5, in zero magnetic field ($H = 0$), the measured value of the effective thermal conductivity is $\lambda_{eff} = 0.189\,\mathrm{W/K\cdot m}$, which shows that λ_{eff} of the

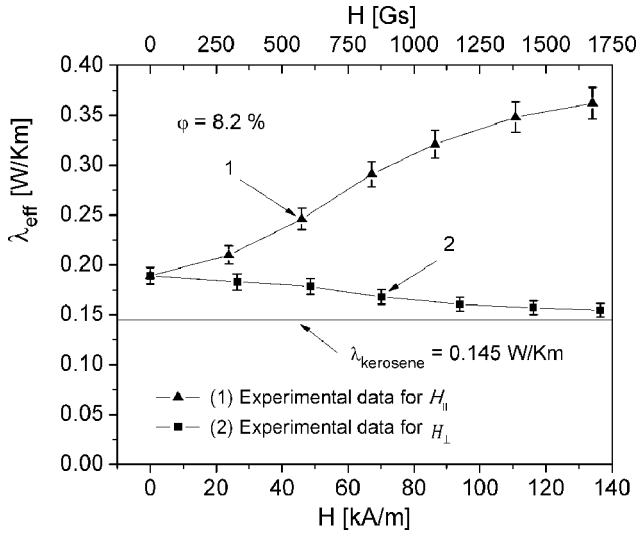

Fig. 5. Plot of the experimental dependence of the effective thermal conductivity, λ_{eff}, of the ferrofluid sample on the magnetic field ($\varphi = 8.20\%$).

ferrofluid increases by 1.30 times compared to the thermal conductivity of kerosene, $\lambda_{ker}(\exp) = 0.145\,\mathrm{W/K \cdot m}$. For a kerosene-based ferrofluid with magnetite particle having a particle concentration of 7.8%, Philip *et al.* [6,10] observed an increase by 1.23 times of the thermal conductivity comparable to the thermal conductivity of the kerosene, in zero magnetic field, similar to our results.

By increasing the intensity of the parallel magnetic field, H_{II} (see fig. 5), λ_{eff} of ferrofluid increases very much. Thereby, at the maximum value of the parallel magnetic field $H_{II,max} = 134\,\mathrm{kA/m}$ (or 1675 G), λ_{eff} increases by 91% in comparison to the value λ_{eff} in zero magnetic field and by 150% with respect to the thermal conductivity of the carrier liquid (kerosene), λ_{ker}. Similar experimental results were obtained by other authors [10, 15,35,36] for similar types of ferrofluids.

When applying the magnetic field, $H_{\perp}$, perpendicular to the temperature gradient (see fig. 5), the effective thermal conductivity, λ_{eff}, of the ferrofluid decreases with increasing the intensity of $H_{\perp}$, tending towards the value $0.154\,\mathrm{W/K \cdot m}$, which is close to the value $\lambda_{ker}(\exp) = 0.145\,\mathrm{W/K \cdot m}$, of the thermal conductivity of the carrier liquid (kerosene). Thus, at the maximum value of the perpendicular magnetic field $H_{\perp,max} = 136\,\mathrm{kA/m}$ (or 1700 Gs), λ_{eff} decreases with 18% in comparison to the value λ_{eff} in zero magnetic field. Similar results were obtained by Vinod *et al.* [14], Quiang Li *et al.* [5,9] who observed little changes in the thermal conductivity of ferrofluids under the influence of the magnetic field, $H_{\perp}$, oriented perpendicular to the temperature gradient.

The increase or decrease of the effective thermal conductivity, λ_{eff}, of the ferrofluid sample, under the action of the magnetic field parallel or perpendicular to the temperature gradient, is correlated to the field-induced microstructures along the magnetic field lines (fig. 2(a) and (b)). These microstructures facilitate or hamper the transfer of the heat flux through the ferrofluid. Thus, in the case of H_{II}, the alignment of the particle agglomerations forms field-induced microstructures, similar to "*conducting rods*", which facilitates the transfer of the heat flux from the hot end to the cold end (fig. 2(a)). This leads to the increase of the effective thermal conductivity, λ_{eff}, with the increase of the strength of field, H_{II} (fig. 5). Also, in the case of $H_{\perp}$, the field-induced microstructures behaves like a "*filter*" which makes it difficult to transfer the heat flux from the hot end to the cold end (fig. 2(b)). This consequently leads to a decrease of the effective thermal conductivity, λ_{eff}, with the increase of the strength of field, $H_{\perp}$ (fig. 5).

4.2 Theoretical model

The theoretical models for computing the effective thermal conductivity of complex nanofluids are based on so-called mixing rules, which use the thermal conductivity of the components and their concentration. For instance, in ref. [18], some of these theoretical models of thermal conductivity are presented (*i.e.*, Maxwell model, Hamilton-Crosser model, Bruggeman model or the effective medium model).

In our experimental arrangement, a suitable mixing rule is that of Sillars, which (apart from the thermal conductivity of the components and their concentration) takes into account the shape of magnetic-field–induced aggregates, as well as their orientation with respect to the temperature gradient. The Sillars equation [26,27] has been firstly used in computing the dielectric permittivity of systems consisting of ellipsoids dispersed in a host medium [26]. In the case of ferrofluids, the Sillars equation written for the theoretical effective conductivity, λ_{theor}, is given by

$$\lambda_{theor} = \lambda_{cl}\left[1 + \frac{1}{A}\cdot\frac{\Phi\frac{A(\lambda_p-\lambda_{cl})}{\lambda_{cl}+A(\lambda_p-\lambda_{cl})}}{1-\Phi\frac{A(\lambda_p-\lambda_{cl})}{\lambda_{cl}+A(\lambda_p-\lambda_{cl})}}\right]. \qquad (3)$$

Here Φ is the volume fraction of the colloidal particles, A is the shape factor of particles, λ_{cl} is the thermal conductivity of the carrier liquid and λ_p is the thermal conductivity of the colloidal particles. Using the following values for these parameters: $\Phi = \varphi = 8.2\%$ (the volume fraction of magnetic particles), $\lambda_{cl} = \lambda_{ker} = 0.145\,\mathrm{W/K \cdot m}$ (the thermal conductivity of kerosene measured by us) and $\lambda_P = \lambda_{mag} = 3.8\,\mathrm{W/K \cdot m}$ (the thermal conductivity of magnetite, value reported in ref. [37]), eq. (3) becomes

$$\lambda_{theor} = 0.145\left[1 + \frac{0.30}{0.145 + 3.355\cdot A}\right]. \qquad (4)$$

In eq. (4), the shape factor A, takes into account the fact that the orientation, shape and eccentricity of particle agglomerations change by applying the magnetic field. Thus, starting from the Sillars equation (3), we have proposed a theoretical model (applied for the first time to a ferrofluid), for the explanation of the effect of magnetic field on the thermal conductivity of ferrofluids.

In the absence of the magnetic field, the magnetic particles in the ferrofluid are considered to be approximately spherical and the shape factor is $A = 1/3$. In this case, from eq. (4) the value $\lambda_{theor} = 0.180$ results, approximately equal to the value experimentally obtained in the zero magnetic field, $\lambda_{eff}(\exp) = 0.189$ (see fig. 5). When applying the magnetic field, the volume fraction of the colloidal particles, Φ, does not change, but the particles reorganize locally and form agglomerations, arranged in field-induced microstructures along the magnetic field lines (see fig. 2) and the form factor, A, changes. The particle agglomerations are elongated in the direction of the magnetic field and the stronger the field, the longer the particle agglomeration. Therefore, under the assumption that the particle agglomerations have ellipsoid forms, the ratio between the major axis and the minor axis of the ellipsoid increases with the increase of the magnetic field strength.

In the case of parallel magnetic field to the tube axis ($H_{II} > 0$), as in fig. 3(a), the shape factor, A_{II}, is given by eq. (5) and λ_{theor} is computed by means of eq. (4), in which A is replaced by A_{II}:

$$A_{II} = \frac{1-e^2}{2e^3}\left[\ln\left(\frac{1+e}{1-e}\right) - 2e\right]. \tag{5}$$

In eq. (5), e is the average eccentricity of agglomerations, given by

$$e = \left[1 - \frac{1}{(a/b)^2}\right]^{1/2}, \tag{6}$$

where a is the semi-major axis and b is the semi-minor axis of one agglomeration, having an ellipsoid form. Taking into account that the ratio (a/b) increases by increasing the magnetic field strength, due to the increase of the length of particle agglomeration, as shown by Bacri and Salin in ref. [38], it results from eq. (5) that A_{II} changes by increasing the parallel magnetic field to the tube axis.

Using the Sillars equation (eq. (4)) and eq. (5) (for the magnetic field oriented parallel to the temperature gradient) we have computed the theoretical dependence of the effective thermal conductivity, $\lambda_{theor\,\parallel}$, depending on the ratio a/b between the semi-major axis, a, and the semi-minor axis, b, of particle agglomerations. The obtained results are presented in fig. 6(a).

By comparing the experimental values of the effective thermal conductivity λ_{eff}, from fig. 5, with the theoretical values $\lambda_{theor\,\parallel}$, from fig. 6(a), we were able to determine for the first time the dependence on the magnetic field H of the a/b ratio, presented in fig. 6(b). The fit of a sigmoid function to this dependence, shows that $a/b(H)$ can be expressed by the relation

$$\frac{a}{b}(H) = 13.01391 - \frac{13.25332}{1+\exp\left(\frac{H-73.22673}{32.50979}\right)} \tag{7}$$

which represents a semi-empirical correlation between ratio a/b and H. From eq. (7) it is observed that for $H = 0$ it results that $a/b = 1.021$ (very close to unity) suitable

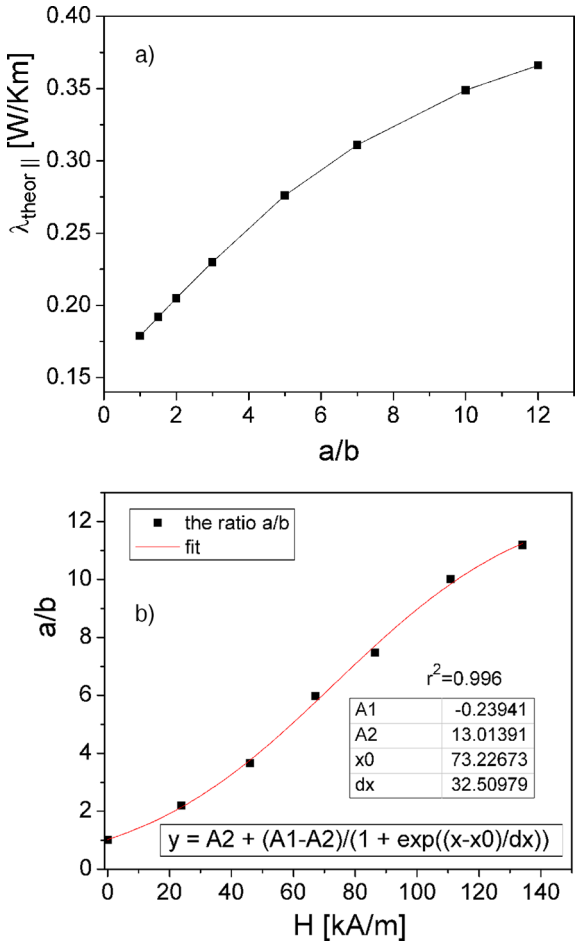

Fig. 6. Theoretical dependence of the effective thermal conductivity of the ferrofluid, $\lambda_{theor\,\parallel}$, on the ratio a/b (a); the ratio a/b as a function of H (b).

to the assumption that in zero magnetic field, the shape of particles is spherical.

Introducing eq. (7) into eq. (6), results in

$$e(H) = \left[1 - \left(13.01391 - \frac{13.25332}{1+\exp\left(\frac{H-73.22673}{32.50979}\right)}\right)^{-2}\right]^{1/2} \tag{8}$$

which indicates the magnetic field dependence of the average eccentricity of particle agglomerations, $e(H)$. As a result, with eq. (5), we can calculate the shape factor A_{II}, as a function of H, $(A_{II}(H))$, taking into account the dependence $e(H)$ of eq. (8); the theoretical effective thermal conductivity $\lambda_{theor,II}(H)$ is computed by means of eq. (4), in which A is replaced by $A_{II}(H)$.

In the case of the magnetic field perpendicular to the temperature gradient, as in fig. 2(b), the shape factor $A_\perp$ is given by following equation:

$$A_\perp = \frac{1-A_{II}}{2}. \tag{9}$$

Equation (9) allows the determination of the shape factor $A_\perp(H)$, knowing the dependence on the magnetic field

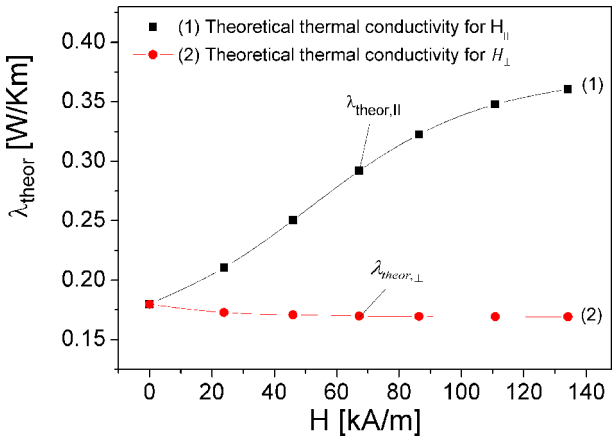

Fig. 7. The dependence of the theoretical thermal conductivity, λ_{theor}, on the parallel (H_{II}) and perpendicular ($H_{\perp}$) magnetic field in relation with the temperature gradient.

of the shape factor $A_{II}(H)$. As a result, the theoretical effective thermal conductivity, $\lambda_{theor,\perp}(H)$, is computed by means of eq. (4), in which A is replaced by $A_{\perp}(H)$. The results obtained for the theoretical effective thermal conductivity, $\lambda_{theor,II}(H)$ and $\lambda_{theor,\perp}(H)$, are presented in fig. 7.

From fig. 7 one can observe that $\lambda_{theor}(H)$ has a similar behaviour to that of the experimental dependence $\lambda_{eff}(H)$, from fig. 5, both for the parallel and perpendicular orientation, of the magnetic field in relation to the gradient temperature. The theoretical thermal conductivity $\lambda_{theor\,\parallel}(H)$ increases with the increase of the magnetic field and the value $\lambda_{theor\,\parallel}$ corresponding of the maximum of magnetic field, $H_{max} = 134\,\mathrm{kA/m}$, is $0.361\,\mathrm{W/K \cdot m}$, being very close to the obtained experimental value, for the effective thermal conductivity, $\lambda_{eff\,\parallel}(\mathrm{exp}) = 0.362\,\mathrm{W/K \cdot m}$ at the same maximum value of the magnetic field. Also, from fig. 7, it is observed that in the case of magnetic field, $H_{\perp}$, oriented perpendicular to the temperature gradient, $\lambda_{theor\,\perp}(H)$ decreases with increasing the intensity of the magnetic field, tending towards the value $0.169\,\mathrm{W/K \cdot m}$, close to the obtained experimental value, $\lambda_{eff\,\perp}(\mathrm{exp}) = 0.154\,\mathrm{W/K \cdot m}$, for the same maximum value of the magnetic field. As a result, the proposed theoretical model based on the Sillars equation, applied for the first time to a ferrofluid shows a good agreement between the obtained theoretical and experimental results regarding the thermal conductivity both in parallel and perpendicular magnetic field with respect to the temperature gradient.

5 Conclusions

In this paper, starting from the conventional thermal conduction method, we have realized a laboratory setup with which we have measured the effective thermal conductivity, of a ferrofluid sample with magnetite particles dispersed in kerosene. The experimental installation was first tested with water and kerosene. The experimental installation allowed us tracking the effect of the external magnetic field intensity on the thermal conductivity of a ferrofluid sample, as well as the effect of direction of the magnetic field relative to the direction of the temperature gradient, on its thermal conductivity.

By applying the perpendicular ($H_{\perp}$) or parallel (H_{II}) magnetic field, to the axis of the tube containing the ferrofluid, λ_{eff} is changed by increasing the intensity of the magnetic field from the λ_{eff} value in zero field. This behaviour either in the $H_{\perp}$ field or in the H_{II} field, with respect to the axis of tube, can be correlated with the formation of particle agglomerations, which are arranged in field-induced microstructures along the magnetic field lines. These field-induced microstructures impede or facilitate the movement of the heat flux from the hot end to cold end of the ferrofluid sample, which thus leads to a decrease or increase of λ_{eff} in the presence of the magnetic field.

To explain the obtained experimental results, we proposed a theoretical model starting from the Sillars equation, applied for the first time to a ferrofluid. In this model we computed the thermal conductivity of the ferrofluid λ_{theor}, taking into account the fact that the shape, eccentricity and orientation of the particle agglomerations change with the strength of magnetic field and its orientation with respect to the axis of the tube in which the ferrofluid is placed.

Assuming that the particle agglomerations have ellipsoid forms and the ratio a/b between the major axis and the minor axis of the ellipsoid increases with increasing of magnetic field strength, the proposed theoretical model allowed us establishing for the first time of a semi-empirical relationship between the ratio, a/b and magnetic field, H.

Both experimental results and theoretical model suggest that ferrofluids are potential candidates for the incorporation in magnetic tuneable heat transfer devices.

CNM and IM acknowledge the partial support from the research contract 02-1-1107-2011/2021 ANCSI-JINR Dubna, items 14 and 81 of the JINR order, no. 269 / 20.05.2020. Also, we express our gratitude to Dr. Aurel Ercuta for fruitful discussions and support in conducting magnetization curve measurements.

Author contribution statement

IM made the experimental configuration for measuring all the samples. CNM and IM designed the research; both authors performed and analyzed the experiments. CNM has developed the theoretical model. CNM and IM supervised the research; both authors have discussed the results and contributed to writing-up the paper.

Nomenclature

H	magnetic field (kA/m) or (G)
H_{II}	magnetic field oriented parallel to the temperature gradient (kA/m)
$H_{\perp}$	magnetic field oriented perpendicular to the temperature gradient (kA/m)
B	magnetic induction (T)
λ_{eff}	effective thermal conductivity (W/K·m)
$\lambda_{eff,II}(H)$	parallel effective thermal conductivity (W/K · m)
$\lambda_{eff,\perp}(H)$	perpendicular effective thermal conductivity (W/K · m)
λ_{theor}	theoretical thermal conductivity (W/K · m)
T_1	temperature of hot source (°C)
T_2	temperature of cold source (°C)
Fe_3O_4	magnetite
NH_4OH	ammonium hydroxide
ρ_F	density of ferrofluid (kg/m^3)
n	particle concentration (m^{-3})
M	magnetization of ferrofluid (kA/m)
M_{∞}	saturation magnetization of the ferrofluid (kA/m)
d_m	mean magnetic diameter of particles (nm)
χ_i	initial magnetic susceptibility
M_S	spontaneous magnetization of the bulk material of magnetite (477.5 kA/m)
φ	volume fraction of the solid phase (%)
φ_m	volume fraction of the magnetic phase (%)
δ	thickness of the non-magnetic shell (nm)
L	length (m)
S	cross-sectional area (m^2)
P_{th}	thermal power (W)
ΔT	temperature difference between the hot end and the cold end (°C)
Δt	time interval (s)
$\mathrm{d}(\Delta T)/\mathrm{d}t$	time derivative of the temperature difference between the hot end and the cold end (°C/s)
C	specific heat capacity of copper (J/kg · K)
λ_{wat}	effective thermal conductivity of water (W/K · m)
λ_{ker}	effective thermal conductivity of kerosene (W/K · m)
Φ	volume fraction of the colloidal particles (%)
A	shape factor of particles
e	average eccentricity of agglomerations
a/b	ratio between the semi-major axis and the semi-minor axis of one agglomeration
A_{II}	shape factor when applying a parallel magnetic field in relation to the temperature gradient
$A_{\perp}$	shape factor when applying a perpendicular magnetic field in relation to the temperature gradient

References

1. S.U.S. Choi, J. Heat Transfer **131**, 033106 (2009).
2. J. Philip, P.D. Shima, Adv. Colloid Interface Sci. **183–184**, 30 (2012).
3. M. Farbod, A. Ahangarpour, Phys. Lett. A **380**, 4044 (2016).
4. R.E. Rosensweig, *Ferrohydrodynamics* (Cambridge University Press, 1985).
5. P.C. Fannin, C.N. Marin, V. Socoliuc, G.M. Istratuca, A.T. Giannitsis, J. Phys. D: Appl. Phys. **36**, 1227 (2003).
6. Mohamad Ali Bijarchi, Mohammad Behshad Shafii, Langmuir **36**, 7724 (2020).
7. Amirhossein Favakeh, Mohamad Ali Bijarchi, Mohammad Behshad Shafii, J. Magn. & Magn. Mater. **498**, 66134 (2020).
8. Mohamad Ali Bijarchi, Amirhossein Favakeh, Mohammad Behshad Shafii, J. Ind. Eng. Chem. **84**, 106 (2020).
9. Q. Li, Y. Xuan, J. Wang, Exp. Therm. Fluid Sci. **30**, 109 (2005).
10. J. Philip, P.D. Shima, B. Raj, Appl. Phys. Lett. **91**, 203108 (2007).
11. A. Gavili, F. Zabihi, T.D. Isfahani, J. Sabbaghzadeh, Exp. Therm. Fluid Sci. **41**, 94 (2012).
12. Mostafa Zarei Saleh Abad, Massoud Ebrahimi-Dehshali, Mohamad Ali Bijarchi, Mohammad Behshad Shafii, Ali Moosavi, Heat Transfer **48**, 2700 (2019).
13. H. Hong, B. Wright, J. Wensel, S. Jin, X.R. Ye, W. Roy, Synth. Met. **157**, 437 (2007).
14. S. Vinod, J. Philip, J. Magn. & Magn. Mater. **444**, 29 (2017).
15. Sithara Vinod, John Philip, J. Mol. Liq. **298**, 112047 (2020).
16. Amir Karimi, S. Salman, S. Afghahi, Hamed Shariatmadar, Mehdi Ashjaee, Thermochim. Acta **598**, 59 (2014).
17. Q. Xue, W.M. Xu, Mater. Chem. Phys. **90**, 298 (2005).
18. W. Duangthongsuk, S. Wongwises, Exp. Therm. Fluid Sci. **33**, 706 (2009).
19. P.M. Hui, X. Zhang, A.J. Markworth, D. Stroud, J. Mater. Sci. **34**, 5497 (1999).
20. X. Wang, X. Xu, S.U.S. Choi, J. Thermophys. Heat Transfer **13**, 474 (1999).
21. R.L. Hamilton, O.K. Crosser, Ind. Eng. Chem. Fundam. **1**, 187 (1962).
22. L. Yang, X. Xu, Int. Commun. Heat Transfer **81**, 42 (2017).
23. N.S. Susan Mousavi, Sunil Kumar, J. Appl. Phys. **123**, 043902 (2018).
24. Dong-Xing Song, Wei-Gang Ma, Xing Zhang, Int. J. Heat Mass Transfer **138**, 1228 (2019).
25. A.R. Challoner, R.W. Powell, Proc. R. Soc. London, Ser. A **238**, 90 (1956).
26. R.W. Sillars, J. Instit. Electr. Eng. **80**, 378 (1937).

27. C.N. Marin, P.C. Fannin, K. Raj, V. Socoliuc, Magnetohydrodynamics **49**, 270 (2013).
28. L. Gabor, R. Minea, D. Gabor, RO Patent No. 108851 (1994).
29. Daniela Susan-Resiga, I. Malaescu, Oana Marinica, C.N. Marin, Physica B: Phys. Condens. Matter **587**, 412150 (2020).
30. I. Mihalca, A. Ercuta, C. Ionascu, Sens. Actuators A: Phys. **106**, 61 (2003).
31. R.W. Chantrell, J. Popplewell, S.W. Charles, IEEE Trans. Magn. **14**, 975 (1978).
32. C.O. Bennett, J.E. Myers, *Momentum, Heat and Mass Transfer*, 3rd edition (McGraw-Hill, New York, 1982).
33. S. Kakaç, A. Pramuanjaroenkij, Int. J. Heat Mass Transfer **52**, 3187 (2009).
34. V. Prakash, V.K. Tyagi, A.K. Tyagi, Nano Vision **6**, 10 (2016).
35. M. Krichler, S. Odenbach, J. Magn. & Magn. Mater. **326**, 85 (2013).
36. M. Ortiz-Salazar, N.W. Pech-May, C. Vales-Pinzon, R. Medina-Esquivel, J.J. Alvarado-Gil, J. Phys. D: Appl. Phys. **51**, 075003 (2018).
37. J. Molgaard, W.W. Smeltzer, J. Appl. Phys. **42**, 3644 (1971).
38. J.C. Bacri, D. Salin, J. Phys. (Paris) Lett. **43**, L-649 (1982).